ISSN 0853-2982

JURNAL TEKNIK SIPIL
Jurnal Teoretis dan Terapan Bidang Rekayasa Sipil

Numerical Simulation of Bed Level Changes Around Structure Due to Waves and Current

Susanna Nurdjaman
Department of Oceanography, Faculty of Earth Sciences and Technology, Institut Teknologi Bandung
E-mail: susanna@fitb.itb.ac.id

Prayoga Aryandi Putra
Department of Oceanography, Faculty of Earth Sciences and Technology, Institut Teknologi Bandung
E-mail: pryga.aryndi@gmail.com

Abstract

Interactions between sediments in the marine environment with the dynamics of the ocean can generate sediment movement. Sedimentation and erosion is the result of these interactions, which often have a negative impact on the harbor waters or coastal environment. The purpose of this research is to understand the process of sediment transport caused by the dynamics of currents and waves on the basis of morphological changes and the potential that can lead to scour for coastal protection structures (groin).Coupled model of hydrodynamic model, spectral wave and sediment transport were conducted to study the pattern of sediment movement. Simulations carried out by varying the waveform specification that propagates to the domain model. Verification of maximum velocity magnitude due to Van Rijn (1987), Nurdjaman and Ningsih (2003), and Adilantip (2012) shows good agreement with the differences value below 5%. While verification of wave height and wave stress radiation with analytical calculation shows good comparison with the mean of differences value 15%. The results of the study indicate that scour depth of 0,955 m was formed at the end of the simulation by the discharge input only. When the discharge combined with the various wave height and periods, scour depth increases by about 3 - 14%. Location of the scour depth coincides with the location of the maximum velocity at the tip of the groin structures to the left side.

Keywords: *Hydrodynamic simulation, simulation of waves, sediment transport, groin structure, scour, and bed level change.*

Abstrak

Interaksi antara sedimen di lingkungan laut dengan dinamika laut dapat menghasilkan pergerakan sedimen. Proses sedimentasi dan erosi merupakan hasil dari interaksi tersebut yang tak jarang berdampak negatif terhadap perairan pelabuhan ataupun lingkungan pesisir. Tujuan dari penelitian ini yaitu untuk memahami proses transpor sedimen yang diakibatkan oleh dinamika arus dan gelombang terhadap perubahan morfologi dasar dan potensinya yang dapat mengakibatkan gerusan terhadap struktur pelindung pantai (groin). Dilakukan model kopel hidrodinamika, gelombang spektral, dan transpor sedimen untuk mempelajari pola pergerakan sedimen. Simulasi dilakukan dengan memvariasikan perbedaan spesifikasi gelombang yang menjalar terhadap domain model. Simulasi dilakukan dengan memvariasikan spesifikasi waveform yang merambat ke model domain. Verifikasi besarnya kecepatan aliran maksimum dari hasil model oleh Van Rijn (1987), Nurdjaman dan Ningsih (2003), dan Adilantip (2012) menunjukkan kesesuaian yang baik dengan perbedaan nilai di bawah 5%. Sedangkan verifikasi tinggi gelombang dan radiasi tegangan gelombang dengan perhitungan analitik menunjukkan perbandingan yang baik dengan rata-rata perbedaan nilai 15%. Hasil penelitian menunjukkan bahwa kedalaman gerusan 0,955 m terbentuk pada akhir simulasi dengan input debit sungai saja. Bila ddebit sungai dikombinasikan dengan berbagai tinggi dan perioda gelombang, kedalaman gerusan meningkat sekitar 3 - 14%. Lokasi kedalaman gerusan bertepatan dengan lokasi kecepatan aliran maksimum pada ujung struktur groin sisi kiri.

Kata-kata Kunci: *Simulasi hidrodinamika, simulasi gelombang, transpor sedimen, struktur groin, dan perubahan morfologi dasar.*

1. Introduction

Ocean dynamics and interactions of the surroundings will always have a reciprocal relationship. One of the phenomena of the interaction dynamics of the ocean and the surrounding environment is a sediment transport process. In waters involving many human interests such as in harbor waters and coastal areas, sediment transport process has an important role in determining the environmental conditions.

Structure such as groin, break water or bridge pier that obstruct or otherwise change the flow pattern in the vicinity of the structure, may cause localized erosion or scour. Changes in flow characteristics lead to changes in sediment transport capacity and thus change the morphology or bed level.

Erosion and deposition of sediment transport is a process that often detrimental to human activity and also has the potential to damage biological resources and non-biological. Erosion becomes a threat when development

Diterima 10 Juli 2017, Direvisi 14 November 2017, Diterima untuk dipublikasikan 31 November 2017.

or human activity involved. The process of construction of a building structure the beach in the coastal areas are at risk because somehow this process can alter the circulation pattern of water flow. When a building is placed in the water area of the building, it will change the surrounding ocean circulation and increase the capacity of local sediment transport (Summer and Fredsøe, 2002). If the process is ongoing, the erosion can undermine the bed level of the foundation structure which ultimately destabilize the beach protection building.

Over the past several years, there has been a rapid expansion of literatures concerning about erosion around structures in both laboratory experiment and numerical simulation (Ouillon and Dartus, 1977; Summer and Fredsoe, 1997a; Summer and Fredsoe, 1997b; Walker, et al., 1991; Kawata and Tsuchiya, 1988; Jyothi, et al., 2002; Nurdjaman and Ningsih, 2003). Simulation of bed level change due to current and wave around groin will be discuss in this paper.

In addition, due to the sedimentation process sediment transport in relation to marine transportation can cause disruption of the marine navigation. If silting navigation canals where the entry of ships, then this it will add to the cost of dredging the canals. Therefore, it is necessary to know information about the phenomenon of sediment transport close to the real condition which is a process that also involves the dynamics of currents and waves.

2. Methodology

Simulation of bed level changes carried out by depth-integrated 2-D model of sediment transport model generated by waves and current. Spectral wave model was used to simulate propagation of static wave in the area to generate current field as the input in hydrodynamic model. While the hydrodynamic model was with used to simulate water circulation (water discharge on inlet and outlet) as the input for the sediment transport model. Finally, sediment transport model was then run to simulate the movement of total sediment (bed load and suspended of non-cohesive sediment transport) in the area in order to simulate bed level changes, especially around structure (single groin).

2.1 Hydrodynamic model

The horizontal movement of currents in the 2-D simulated by Mike 21 Flow Model FM. Governing equations in this model using the equations of continuity and momentum equations (Navier-Stokes). Both equations are integrated to depth in order to obtain 2-D hydrodynamic equations in shallow waters as follows (an adaptation from DHI Water & Environment, 2012a):

The continuity equation is:

$$\frac{\partial \eta}{\partial t} + \frac{\partial uh}{\partial x} + \frac{\partial vh}{\partial y} = \frac{\partial h}{\partial t} \quad (1)$$

The momentum equations (*Navier-Stokes)* are:

x-axis direction:

$$\frac{\partial u}{\partial t} + u\frac{\partial u}{\partial x} + v\frac{\partial u}{\partial y} = -g\frac{\partial \eta}{\partial x} + \frac{1}{\rho h}\left(\frac{\partial S_{xx}}{\partial x} + \frac{\partial S_{xy}}{\partial y}\right) + \frac{gu\sqrt{u^2 + v^2}}{C^2 h} + A_H\left(\frac{\partial^2 u}{\partial x^2} + \frac{\partial^2 u}{\partial y^2}\right) \quad (2)$$

y-axis direction:

$$\frac{\partial v}{\partial t} + u\frac{\partial v}{\partial x} + v\frac{\partial v}{\partial y} = -g\frac{\partial \eta}{\partial y} + \frac{1}{\rho h}\left(\frac{\partial S_{yx}}{\partial x} + \frac{\partial S_{yy}}{\partial y}\right) + \frac{gv\sqrt{u^2 + v^2}}{C^2 h} + A_H\left(\frac{\partial^2 v}{\partial x^2} + \frac{\partial^2 v}{\partial y^2}\right) \quad (3)$$

with :

η : surface elevation (m)

h : total depth (m)

u, v : current velocity, in x-axis and y-axis direction, respectively (m/s)

g : gravitational acceleration (9,8 m/s^2)

ρ : sea water density (kg/m^3)

$S_{xx}, S_{xy}, S_{yx}, S_{yy}$: component stress radiation due to wave presence (S_{xy}) means the stress radiation component which working perpendicular to *x*-plane and unidirectional with *y*-axis (kg/m s^2)

C : chezy coeficient (m$^{1/2}$/s)

A_H : eddy viscosity (m^2/s)

2.2 Spectral wave model

In this study, wave model simulated wave MIKE21 SW software. Wave dynamics in the study follows the wave action density equation where the action density, N (σ, θ), and wave energy, E (σ, θ), have relationships as:

$$N = \frac{E}{\sigma} \quad (4)$$

with:

N : wave action density

E : wave energy

σ : relative angular frequency

The solution to the wave action density can be solved by following equations in the adoption of DHI Water and Environment (2012b):

$$\frac{\partial N(\sigma,\theta;\, x,y,t)}{\partial t} + \frac{\partial c_x N(\sigma,\theta;\, x,y,t)}{\partial x} + \frac{\partial c_y N(\sigma,\theta;\, x,y,t)}{\partial y} + \frac{\partial c_\theta N(\sigma,\theta;\, x,y,t)}{\partial \theta} + \frac{\partial c_\sigma N(\sigma,\theta;\, x,y,t)}{\partial \sigma} = \frac{SE(\sigma,\theta;\, x,y,t)}{\sigma} \quad (5)$$

with:

$N(\sigma,\theta;\, x,y,t)$: wave action density (m^{2}s/rad)

Diterima 10 Juli 2017, Direvisi 14 November 2017, Diterima untuk dipublikasikan 31 November 2017.

c_x and c_y : group velocity, *x*-axis and *y*-axis direction, respectively (m/s)

c_θ : wave group velocity representing changes of wave direction, θ (m/s)

c_σ : wave group velocity representing changes of relative angular frequency (m/s)

SE : source term for the energy balance equation

θ : the direction of wave propagation

Wave action density equation has the function of the source (SE), which represents the growth and/or energy dissipation. The function source (SE) is a superposition of energy sources that describe various physical phenomena.

The energy is divided into several sections which are growing due to wind stress (SE_{in}), dissipation due to white capping (SE_{ds}), wave energy transfer due to non-linear interaction of waves (SE_{nl}), wave energy dissipation due to bed friction (SE_{bot}), and wave energy dissipation due to wave breaking (SE_{surf}). In this study involved only a function of source resource function of wave energy dissipation due to friction base, so the equation superposition source function can be written as follows:

$$SE = SE_{bot} \tag{6}$$

Dissipation caused by bed friction base, defined as:

$$SE_{bot}(\sigma,\theta) = -\frac{\left(C_f + \frac{f_c\left(\overline{u\,k}\right)}{k}\right) k\, E(\sigma,\theta)}{\sinh 2kh} \tag{7}$$

with C_f coefficient of friction, f_c the coefficient of friction for the current, u is the velocity, and h water depth. Initial value of f_c is 0, while the value C_f has a range between 0.001 to 0.01 m/s.

Diffraction phenomenon in SW MIKE21 model is modeled by using a refraction-diffraction approach. Wave propagation in shallow water with the contained flow field, the speed of propagation of the wave group spatially $(c_x, c_y, c_\sigma, c_\theta)$ is corrected to the given diffraction by the following equation (Holthuijsen, et al., 2007, in DHI Water and Environment, 2012b):

$$\left(c_x, c_y\right) = c_g{}' + U = c_g(1 + \delta_A) + U \tag{8}$$

$$c_\sigma = \frac{\partial\sigma}{\partial h}\left[\frac{\partial h}{\partial t} + U\left(\frac{\partial h}{\partial x} + \frac{\partial h}{\partial y}\right)\right] - c_g'.k\frac{\partial U}{\partial s} \tag{9}$$

$$c_\theta = c_g'\left(\frac{1}{k}\frac{\partial k}{\partial m} + \frac{1}{2(1+\delta_a)}\frac{\partial \delta_A}{\partial m}\right) \tag{10}$$

with δ_a is diffraction dimensionless parameter which defined by:

$$\delta_A = \frac{\nabla\, cc_g\, \nabla A}{k^2 cc_g\, A} \text{ dengan } \nabla\, cc_g\, \nabla A = \frac{\partial}{\partial x}\left(cc_g\frac{\partial A}{\partial x}\right) + \frac{\partial}{\partial x}\left(cc_g\frac{\partial A}{\partial y}\right) \tag{11}$$

with:

k : wave number

A : wave amplitude

$c_g, c_g{}'$: wave group velocity with and without the effect of diffraction, respectively

c : wave phase velocity without the effect of diffraction

In simulating wave model in shallow water with wave reflection phenomenon, the presence of structures need to be considered. In some cases, the phenomenon of reflection can be ignored as the sandy beach where the value of reflection is not significant (Holthuijsen, 2007). Incident wave which reflected by structure follows a reflection coefficient, K_r. The value of K_r, mathematically follows the following equation:

$$K_r = \frac{H_r}{H_i} \tag{12}$$

According to Reeve, et al. (2004), the value of the reflection coefficient has its own value ranges for each structural material. In this study, because the structure is assumed impermeable concrete wall and reflected wave came not perfectly, then the value of the reflection coefficient is 0.7 (the concrete wall has a reflection coefficient value range of 0.7 to 1).

Calculation of the reflection phenomenon is usually not separated by the transmitted wave and the absorbed wave by the structure. So that the reflection phenomenon in its calculation involves three consecutive coefficients, they are reflection coefficient (K_r), transmition coefficient (K_T), and absorbance coefficient (K_L), which mathematically arranged in the following equation (adopted from DHI Water and Environments, 2012b):

$$K_r^2 + K_T^2 + K_L^2 = 1 \tag{13}$$

2.3 Sediment transport model

Sediment transport model was simulated with an add-on applications on MIKE 21 Flow Model, sand transport module. Sediment transport model calculations generated by a combination of currents and waves is calculated by involving stress wave radiation to the calculation of the resultant flow.

Calculation of total sediment transport is the sum of bed load sediment transport and suspended sediment transport. Mathematically the calculation of bed load sediment transport as follows (MIKE DHI Water and Environment, 2012c):

$$q_b = 5p\left(\sqrt{\theta'} - 0.07\sqrt{\theta_{cr}}\right)\sqrt{(r_s - 1)gd} \text{ if } \theta' > \theta_{cr} \tag{14}$$

p is the probability of which all the particles will, θ' is the dimensionless shear stress (Shields parameter), and θ_{cr} is critical when particles moves, and s the relative density of the bed load material.

p is defined as:

$$p = \left[1 + \left[\frac{\frac{\pi}{6}b}{\theta' - \theta_{cr}}\right]^4\right]^{-\frac{1}{4}} \tag{15}$$

Diterima 10 Juli 2017, Direvisi 14 November 2017, Diterima untuk dipublikasikan 31 November 2017.

b is the coefficient of dynamic friction. While shear stress (Shields parameter) is defined as:

$$\theta' = \frac{U_f{}^2}{(r_s - 1)gd} \quad (16)$$

U_f is the friction velocity due to flow-wave can be expressed mathematically as follows (adaptation DHI Water & Environment, 2012c):

$$U = \frac{U_f}{\kappa} \ln\left(\frac{\frac{k_N}{30} + \delta}{\frac{k_N}{30}}\right) \quad (17)$$

with :

κ : von Karman constant

U : depth average velocity (m/s)

U_f : near-bed friction velocity (m/s)

k_N : bed roughness

δ : thickness of boundary layer

Suspended sediment tranport calculation, mathematically expressed by the following equation (Engelund and Fredsøe 1976 in DHI MIKE Water and Environment, 2012c)

$$q_s = 11{,}6\, U_f c_b a\left(I_1 \ln\left(\frac{30h}{k_N}\right) + I_2\right) \quad (18)$$

c_b is the bed concentration of suspended sediment at a = 2d = reference level for c_b, I_1 and I_2 is integral Einstein, h is the water depth, and k_N is a bed roughness. Value of c_b can be defined as:

$$c_b = \frac{0{,}65}{\left(1 + \frac{1}{\lambda}\right)^3} \quad (19)$$

which λ is linear concentration defined as:

$$\lambda = \sqrt{\frac{\theta' - \theta_{cr} - \frac{\pi pb}{6}}{0.027 r_s \theta'}} \quad \text{if } \theta' > \theta_{cr} + \pi pb/6 \quad (20)$$

Integral I_1 and I_2 respectively are integration function of dimensionless reference level $(a_r = a/h)$ and from *Rouse* number:

$$R_O = \frac{w_o}{\kappa U_f} \quad (21)$$

w_o is fall velocity. The value of I_1 and each integrable on the interval z = a to z = h, which z measured from bottom.

2.4 Bed level changes calculation

Calculation of bed level changes, mathematically following equation as below:

$$\frac{\partial z_b}{\partial t} + \frac{1}{1 - n_s}\left(\frac{\partial q_x}{\partial x} + \frac{\partial q_y}{\partial y}\right) = 0 \quad (22)$$

With z_b is bed level, q_x and q_y respectively are total sediment transport in x-axis and y-axis, and also n_s is porosity (empty space in the overall sediment grains).

2.5 Numerical solution

Method of numerical solution of model to solve spatial domains using finite volume method. This finite volume method is based on numerical resolution by discretizing the integral form of the equation, not the discretization of its differential form (Wendt, 2009). In finite volume methods, spatial domains are divided into cells that cover the entire domain. The model uses triangular (triangular) cells and forms an unstructured mesh. Hydrodynamic variables at discrete points in cells are called nodes. The nodes used in the model are at the center of the cell (cell-centered). The cell-centered formulation nodes assume that the value of the bound variable present in the cell is the average value of the variable in that one cell.

3. Model Application

3.1 Model area

The study area is the open canals synthetic domain with structures groins are installed perpendicular to the edge of the canal. Domain models in this study is similar to the model of open channels on Van Rijn (1987), with a length of 3100 m and a width of 100 m. There is a groin domain models in the domain of the model with the length and width respectively 400 m and 100 m. Uniform bathymetry value at each point of the mesh with a depth of 6 m.

3.2 Simulation design

In this study, some scenarios were conducted which aims to look at the behavior of currents and waves on the rate of sediment transport and bathymetry changes. The models were simulated for 24 hours. Generally, the scenario models divided into two parts, hydrodynamic-sediment transport model and hydrodynamic-wave-sediment transport model.

In simulating sediment transport and the bed level changes model, there are some parameters that are required as input data for the model refers to a model Van Rijn (1987). Specification of input data types of sediment can be seen in **Table 1**.

Domain model for hydrodynamic model simulation, wave model, and sediment transport model can be seen in **Figure 1**. In the model domain in **Figure 1** there are three boundary conditions i.e on the left of domain model is open boundary (inlet), on the right domain model is open boundary condition (outlet), on the top and botton of the domain model is close boundary. The domain area is composed by mesh irregularities. Open boundary conditions are located along the coordinates (0, 0-1000) and (3100, 0-1000). The bathymetry value is uniform at each mesh point with a depth of 6 m.

Diterima 10 Juli 2017, Direvisi 14 November 2017, Diterima untuk dipublikasikan 31 November 2017.

Table 1. Input data for bed level changes model

Parameter	Simbol	Value	Unit
Sediment Density	ρ_s	2.650	kg/m^3
Water Density	ρ	1.000	kg/m^3
Von Karman Constants	κ	0,4	-
Porosity of Bed Material	p	0,4	-
Water Temperature	T	10	˚C
Chezy Coefficient	C	41,139	m$^{1/2}$/s
Diameter of Bed Material	d_{50}	0,2	mm
Critical Shields Parameter	θ_{cr}	0,045	-

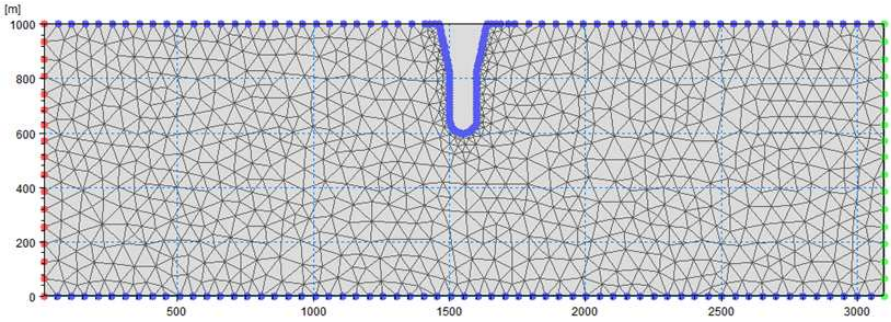

Figure 1. Domain of synthetic model

Simulation of bed level changes changes in the study were divided on the forces generating sediment transport. This study conducted three scenarios, those are bed level changes due to flow, flow with the variance of wave height, and flow with the variance of wave periods. At inlet was set up discharge with 4000 m3/s, while at the outlet there is no change of depth during simulation. Wave height was first varianced with current combined at inlet, respectively 0.1 m and 0.5 m. While wave periodes varianced at inlet with respectively 8 s, and 15 s. In addition, a wave that propagates into the model domain is assumed not to undergo a breaking wave and propagating direction forming an angle of 0˚ to the current at the inlet.

4. Results and Discussion

4.1 Model verification

4.1.1 Hydrodynamic model

Input data in the form of discharge inflow at the outlet with a magnitude of 4000 m3/s generates an average velocity of 0.65 m/s along the canal mouth. Calculation of average velocity along the mouth of the canal is done by calculating the average value of the velocity with respect to time in each of its mesh cells and also averaging its velocity as a function of the space (along the mouth of the canal).

Significant differences of elevation in the front left part of the head groins accelerate the maximum current speed. The maximum velocity occurs on the left side of the head of the groin (upstream region) with a magnitude of 1.74 m/sec. Verification of hydrodynamic model simulation results obtained by comparing the value of the parameters of previous studies which have been carried out Van Rijn (1987), Nurdjaman and Ning (2003), and Adilantip (2012) (see **Table 2**).

Table 2. Verification result of maximum current velocity (input discharge)

Parameter	1	2	3	4	Relative Differences		
	MIKE 21	Van Rijn (1987)	Nurdjaman and Ningsih (2003)	Adilantip (2012)	$P_{1\text{-}2}$	$P_{1\text{-}3}$	$P_{1\text{-}4}$
Maximum Velocity (*depth-averaged*) (m/s)	1,74	1,72	1,81	1,72	1,16%	3,87%	1,16%

Verification of maximum velocity (input discharge) shows the flow pattern similar to hydrodynamic models that have been carried out by Van Rijn (1987) (see **Figure 2** and **Figure 3**). When the current approached groin, current turned toward the head of groin because it was blocked by structures. As a consequence there is accumulation of the mass of water which resulted in an increase of water level.

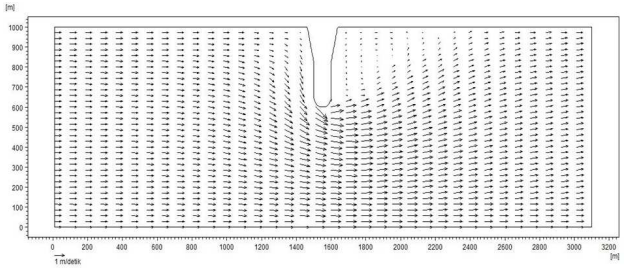

Figure 2. Streamline pattern as result of hydrodynamic model (discharge)

Diterima 10 Juli 2017, Direvisi 14 November 2017, Diterima untuk dipublikasikan 31 November 2017.

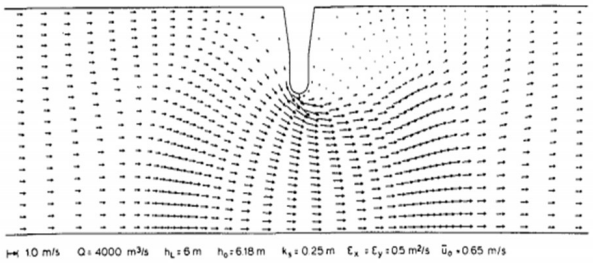

Figure 3. Streamline pattern as result of hydrodynamic in 24 hours by Van Rijn (1987)

Intensification of the current at the head of the groin caused by a narrowing topography. This narrowing topography cause a cumulation of water masses, resulting in differences of relatively higher elevation which impact on increasing the velocity. The location of the maximum velocity indicated by streamline on Van Rijn (1987) the simulation results is located to the left of the head of the groin (see **Figure 3**). The same result is indicated by the simulation results in **Figure 2** which is the maximum velocity vector at the left of the head of the groin.

4.1.2 Spectral wave model

Verification results of wave modeling is done by comparing the output parameters wave model with the analytic calculation. To see a comparison of the analytical calculation, then made several points overview which is done involving one direction analytical only. Locations that serve as points of reviews for the verification that are at y = 570 m and respectively at x = 450 m and x = 1370 m (here in after respectively referred to as point 1 and point 2). The points of the review is on the upstream area where the phenomenon of diffraction and reflection waves due to groin structure has not happened.

Parameters of wave model results were compared to the analytical calculation of which are the wave height and wave radiation stress. Wave model verification scenario can be seen in **Table 3**. The percentage difference relative to the significant wave height produces reasonably good value at under 20%. For verification stress wave radiation, the relative differences between models and analytical calculations are still quite good agreement.

4.2 Simulation Results

4.2.1 Surface water simulation pattern

Discharge inflow with magnitude 4000 m3/s at the open boundary condition causes the highest water level along the canal mouth which equal to 0.14 m (see **Figure 4** below). In **Figure 4**, it appears that there is a significant elevation gradient near the upstream area, on the left groin cause speed acceleration. The minimum elevation occurred in front of the head groin structure which at -0.14 m.

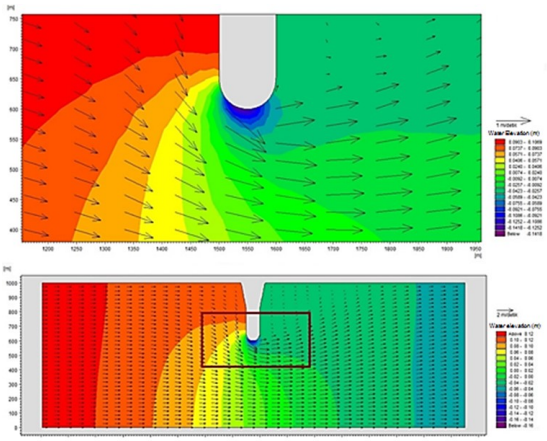

Figure 4. Streamline pattern and surface elevation as a result of hydrodynamic model simulation

Table 3. Verification of wave model

Parameter	Point 1		Point 2		Relative Differences between Model and Analytical Calculations		
	Model	Analytical	Model	Analytical	Point 1	Point 2	Average
Significant Wave Height (H_{mo}) (m)	0.540	0.577	0.456	0.527	6.52%	13.58%	10.05%
Stress Radiation							
Perpendicular to x-plane and directional to x-axis (S_{xx}) (m^3/s^2)	0.234	0.274	0.159	0.229	14.57%	30.82%	22.69%
Perpendicular to y-plane and directional to y-axis (S_{yy}) (m^3/s^2)	0.074	0.066	0.052	0.054	11.26%	3.89%	7.57%

Diterima 10 Juli 2017, Direvisi 14 November 2017, Diterima untuk dipublikasikan 31 November 2017.

On the right side of the groin, movement of currents seem spinning by eddies. The current turbulence on the right side of the groin caused by differences in velocity lateral direction. It appears that in the recirculation zone there is a weak current speed which indicated by a small current vector.

The presence of current-waves combined, generated at the inlet with discharge 4000 m3/s and wave height 0.6 m and period 10 seconds resulted in an average velocity of 0.64 m/sec at along the canal mouth. The maximum current speed recorded during simulation is 1.742 m/ sec. This result show an increase in current magnitude 0.05% compared with the maximum velocity in the scenario of input discharge.

Then the next scenarios, data input of current-waves combined was generated at the inlet with discharge 4000 m3/s and wave height 2.4 and a period 10 seconds resulting average value of current along the mouth of the canal by magnitude 0.65 m/sec and accelerating maximum current speed 1.757 m/sec which is an increase 1.14% compared to the magnitude of the input discharge at the inlet. From the results it appears that the larger the wave height entered the model, the more acceleration of the current velocity as it seen from the result of simulations.

While the input data in the form of discharge and wave with discharge 4000 m3/s and wave height 0.6 m, period 5 seconds resulting an average velocity along the mouth of the canal 0.64 m/sec. These conditions accelerates the maximum velocity to a magnitude 1.742 m/sec which is an increase 0.05%. When the same magnitude of discharge and wave height 0.6 m with periods of 20 seconds was generated at the inlet, it shows that the maximum velocity become 1.741 m/sec, whereas the average speed of currents along the mouth of the canal by 0,65 m/s, this shows that the velocity magnitude increased by 0.11%. The comparison between all of the scenarios summarized in **Table 4**.

4.2.2 Wave field distribution

Simulation models of the wave with a significant wave 0.6 meters and a period 10 seconds generated at the inlet (left boundary), resulting wave height distribution which can be seen in **Figure 5**. The results from this wave model simulations show that during the wave propagation to the outlet, the significant wave height decreases (see **Figure 5**). Wave height values are shrinking as it propagate from its generation place caused by the energy dissipation due to bed friction.

On the left side of the body groin, can be seen that there are wave reflections phenomenon which incident wave is reflected back, so the wave height around left groin body looks relatively different due to the superposition of the incident wave and reflection wave. Region with greater wave height (colored orange in **Figure 5**) has an average height wave height of 0.48 m.

Shadow zone is the area downstream to the right of the body groin is the area most minimal wave height due to decrease in wave energy that hindered by the structure of the groin. Appears in **Figure 5** that in the shadow areas, there has been a process of diffraction which wave energy spread laterally towards the area with lower wave heights, it is indicated by the vector direction of wave propagation which turned toward the area of the shadow zone.

Then another wave height with a height 2.4 m and a period 10 seconds generated along the inlet. Wave propagation to the same period produces wave height relatively greater in magnitude than the surrounding area. The phenomenon occurs due to the reflection process at the left groin structure, the wave height has a mean height 2.25 m.

When generated a significant wave height 0.6 m with a period 5 seconds at inlet, it shows different patterns with the pattern of wave field with wave heights were

Table 4. Comparison parameter of maximum velocity occurred in hydrodynamic simulation

Scenario	Maximum Current Velocity *(Depth-Averaged Velocity)* (m/s)	The Percentage Increase in Maximum Current Velocity Compared to Discharge Scenario
Discharge ($Q = 4000\ m^3/s$)	1.740	-
Discharge with Waves ($Q = 4000\ m^3/s$, H=0.1 m , T= 10 s)	1.741	0.05%
Discharge with Waves ($Q = 4000\ m^3/s$, H=0.6 m , T= 10 s)	1.760	1.14%
Discharge with Waves ($Q = 4000\ m^3/s$, H=0.1 m , T= 5 s)	1.741	0.05%
Discharge with Waves ($Q = 4000\ m^3/s$, H=0.1 m , T = 20 s)	1.742	0.11%

Diterima 10 Juli 2017, Direvisi 14 November 2017, Diterima untuk dipublikasikan 31 November 2017.

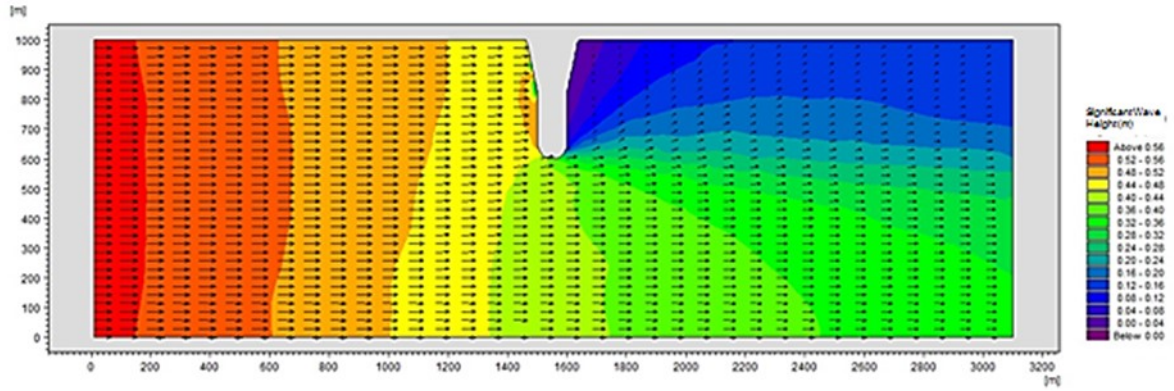

Figure 5. Wave field with wave height of 0.6 m and period of 10 seconds generated at inlet

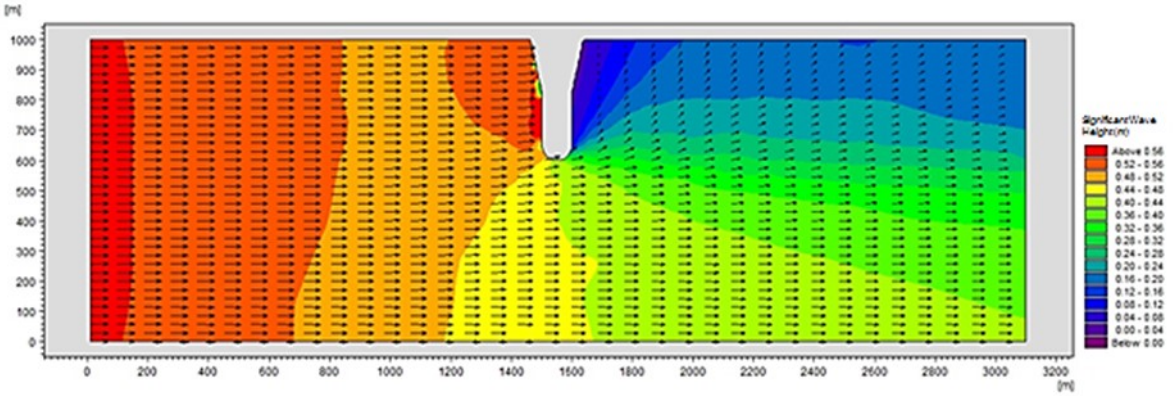

Figure 6. Wave field with wave height of 0.6 m and period of 5 seconds generated at inlet

varianced. The process of reflection on the left groin structure clearly visible. In the **Figure 6** the process is indicated by the wave height relatively greater than the surrounding area which has a mean significant wave height 0.56 m, besides that there are some wave which wave height is relatively low, it happens likely to be caused by the superposition of waves due to reflections.

Specifications of different wave periods tested the significant wave height 0.6 m and periods 20 seconds which generated at the open boundary conditions. This scenario caused different pattern of wave field. This means that the difference between the wave period shows different wave height distribution.

4.2.3 Sediment load and bed level changes distribution

The rate of deposition and erosion rate is related to the velocity friction which stir dimensionless shear stress (Shields parameter). If the Shields parameters that are calculated exceed the critical Shields parameter, then the sediment will move, otherwise the sediment will not move.

Bed level change at the end of discharge input only of hydrodynamic simulation shows the scour around the head of the groin. The maximum scour hole occurred around the head of the left groin (see **Figure 7**) with scour depth of 0.955 m. Sedimentation resulting in silting depth ensued on the right side of the head of the groin. Shallowest bed level value as a result of the maximum deposition process that has a value of 5.009m. The rate of erosion and deposition rate after the model has stabled have a maximum value, each of them are 96.076 mm/hour and 113.442 mm/hour.

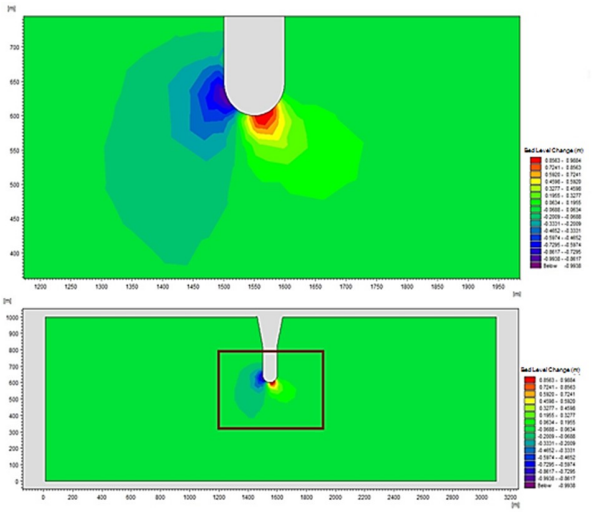

Figure 7. Two dimension profile of bed level changes at the end of simulation of discharge input

In the case of current and wave combined, calculation of bed level changes made by calculating the sediment transport processes which force generator is a resultant flow from the discharge and the wave radiation stress.

Diterima 10 Juli 2017, Direvisi 14 November 2017, Diterima untuk dipublikasikan 31 November 2017.

When discharge and wave height of 0.6 m and period 10 s, the result shows that the maximum rate of erosion in the resultant of discharge and radiation stress has a magnitude of 100.44 mm/h, while the maximum deposition rate of 102.40 mm / hour. This happens because the mathematical equations of bed level changes that move sediment is simply as the total current (current resultant) when the near bed velocity exceeds the critical Shields parameter. The maximum erosion rate on this scenario increase scour hole by 4.19% compare to the discharge input scenario.

Current and wave radiation generation on sediment transport also appears to be more significant on erosion and deposition process which is indicated by the increase and silting around the structure. Scour occurs on the left of head groin with scour hole maximum is 0.995 m. In other words, the presence of a wave with wave height 0.6 m and period 10 seconds increases the scour hole at 4.18%.

Bed level changes with the driving forces in the form of currents and waves with a height 2.4 m and period 10 seconds yielding that the maximum erosion rate of 100.906 mm / hour which has been increased scour hole of 14.76% compare to scenario of discharge input, while maximum deposition rate is 93.444 mm / hour.

The presence of a wave with smaller period 5 seconds and wave height 0.6 m in the sediment transport model of wave-current combined produces the amount of radiation that produces stress that is not too different. Although not so different, but its wave height/wave energy distribution on space occured because it is influenced by wave velocity (a function of the period). It yield maximum erosion rate scenarios magnitude of 100.33 mm /hour, which means there has been increased scour hole compared to discharge input scenario to 4.18%. Meanwhile, the maximum deposition rate on this scenario is 100.330 mm /hour.

Sediment transport model combination of currents and wave with a wave height 0.6 m and a period 20 seconds produce the maximum erosion rate with a magnitude of 100.33 mm/h, while the maximum deposition rate of 93.44 mm/hour. Scour ensued left side with the head groins scour hole to a maximum 0.990 m or an increase up to 3.66% scour hole compared to the case with the input data discharge. **Table 5** presents the depth of scour holes that are formed for each scenario.

Table 5. Scour depth formed on each scenarios

Scenario	Scour Depth (m)	The Percentage Increase in Scour Depth Compared to Discharge Input Scenario
Discharge (Q = 4000 m^3/s)	0,955	-
Discharge and Waves (Q = 4000 m^3/s, H=0.1 m , T= 10 s)	0,995	4,19%
Discharge and Waves (Q = 4000 m^3/s, H=0.4 m , T= 10 s)	1,096	14,76%
Discharge and Waves (Q = 4000 m^3/s, H=0.1 m , T= 5 s)	0,995	4,19%
Discharge and Waves (Q = 4000 m^3/s, H=0.1 m , T = 20 s)	0,990	3,66%

5. Conclusions

1. Verification result of maximum current velocity that occurred during discharge input simulation produce a fairly good relative difference to the previous study (Van Rijn, 1987; Nurdjaman and Ning, 2003; and Adilantip, 2012), with an average relative difference below the value of 5%.

2. Verification result ofc wave height to its analytical calculation yield relative difference below 15%. The relative differences of wave radiation stress parameter has an average value of 15%.

3. The current pattern does not change when there is a wave of the presence propagating paralel to the direction of flow, but the magnitude of the depth average current increase when the stress wave radiation is taken into account. The maximum velocity is located in the head of the left groin (upstream area). The percentage increase in the maximum velocity magnitude when there is the presence of the wave.

4. The wave field with wave height input data varied, causing greater wave energy, this impact to the greater of wave height. While the wave model with wave period input data varied showed a different pattern of energy distribution. Both of these affect the distribution and magnitude of the stress wave radiation.

5. The position of the maximum scour or erosion occurs in the domain model is close to the tip of the head of the left groin in the upstream area. While the position of the maximum deposition occurs on the right side of the head or in the groin area downstream.

6. The addition of wave height causes increase in deposition rate and the erosion in the domain model where this impact on the scour depth formed in the end of the simulation scenarios.

7. Scour depth formed at the end of the simulation in the case of the input data of discharge is 0.955 m. The presence of the waves successively increased impact on scour depth, especially the effect of greater wave height.

Diterima 10 Juli 2017, Direvisi 14 November 2017, Diterima untuk dipublikasikan 31 November 2017.

References

Adilantip, A.H.P., 2012, *Model Numerik Gerusan Lokal di Sekitar Struktur,* Tugas Akhir, Program Studi Oseanografi, ITB, 2012.

DHI Water *and* Environment, 2012a, *MIKE 21& MIKE 3 FLOW MODEL FM: Hydrodynamic and Transport Module Scientific Documentation,* DHI, Agem Alle 5, DK-2970 Hersholm, Denmark.

DHI Water *and* Environment, 2012b, *MIKE 21: Spectral Wave Module Scientific Documentation,* DHI, Agem Alle 5, DK-2970 Hersholm, Denmark.

DHI Water *and* Environment, 2012c, *MIKE 21: Sand Transport Module Scientific Documentation,* DHI, Agem Alle 5, DK-2970 Hersholm, Denmark.

Holthuijsen, L.H., 2007, *Wave in Ocean and Coastal Waters*, Cambridge, New York.

Jyothi, K., Mani, J.S., and M.R. Pranesh, 2002, Numerical Modeling of Flow around Coastal Structure and Scour Prediction, *Ocean Engineering* 29 (2002) 417 – 444.

Kawata, Y., and Y. Tsuchiya, 1988, Local Scour Around Cylindrical Piles Due To Waves and Currents Combined*, Coastal Engineering chapter* 97 (1988) 1310 - 1322.

Nurdjaman, S., dan N.S. Ningsih, 2003, *Numerical Simulation of Local Scour around Groins,* The-12th Indonesian Scientific Meeting, Osaka University, September 6-7, 2003.

Ouillon, S., dan D. Dartus, 1977, Three-Dimensional Computation of Flow Aroudn Groyne, *Journal Hydraulic Engineering*, Vol. 123, p962-970.

Reeve, D., Chadwick, A., dan C. Fleming, 2004, *Coastal Engineering: Processes, Theory, and Design Practice,* Spon Press, Oxon, Canada, ISBN 0-203-67558-4.

Summer, B.M., dan J. Fredsøe, 1997a, Scour at the Head of Vertical-wall breakwater*, Coastal Engineering*, vol. 29, 201-230.

Summer, B.M., dan J. Fredsøe, 1997b, Scour at Round Head of A Rubble-Mound Breakwater*, Coastal Engineering*, vol. 29, 231-262.

Summer, B.M., and J. Fredsøe, 2002, The Mechanics of Scour in the Marine Environment*, Advanced Series on Ocean Engineering* – Volume 17, World Scientific., ISBN 981 – 02 – 4930 – 6.

Van, Rijn, L.C., 1987, *Mathematical Modelling of Morphological Processes in the Case of Suspended Sediment Transport,* Thesis approved by Delft University of Technology. Delft Hydraulics Communication. No. 382.

Walker, D.J., Dong, P., and K. Anastasiou, 1991, Sediment Transport Near Groynes in the Near-shore Zone, *Journal of Coastal Research*, p1003-1011, Fort Lauderdale, Florida.

Wendt, J.F., 2009, *Computational Fluid Dynamics,* Springer-Verlag Berlin Heidelberg, German.

Diterima 10 Juli 2017, Direvisi 14 November 2017, Diterima untuk dipublikasikan 31 November 2017.